Atmosphere **2015**, *6*, 273-298; doi:10.3390/atmos6030273

OPEN ACCESS

atmosphere

ISSN 2073-4433

www.mdpi.com/journal/atmosphere

Article

Effects of Aerosol on Cloud Liquid Water Path: Statistical Method a Potential Source for Divergence in Past Observation Based Correlative Studies

Ousmane Sy Savane [1,*], Brian Vant-Hull [2], Shayesteh Mahani [2] and Reza Khanbilvardi [2]

[1] Earth and Environmental Sciences Department, Graduate Center, The City University of New York, New York, NY 10031, USA

[2] Cooperative Remote Sensing Science and Technology (CREST) Institute, City University of New York, New York, NY 10031, USA; E-Mails: brianvh@ce.ccny.cuny.edu (B.V-H.); mahani@ce.ccny.cuny.edu (S.M.); rk@ce.ccny.cuny.edu (R.K.)

* Author to whom correspondence should be addressed; E-Mail: Osysavane8@gmail.com; Tel.: +1-917-744-4956.

Academic Editor: Toshihiko Takemura

Received: 11 November 2014 / Accepted: 5 February 2015 / Published: 10 March 2015

Abstract: Studies show a divergence in correlation between aerosol and cloud proxies, which has been thought of in the past as the results of varying physical mechanisms. Though modeling studies have supported this idea, from an observational standpoint it is difficult to attribute with confidence the correlations to specific physical mechanisms. We explore a methodology to assess the correlation between cloud water path and aerosol optical depth using Moderate-resolution Imaging Spectroradiometer (MODIS) Aqua retrieved aerosol and cloud properties for absorbing and non-absorbing aerosol types over land and over the Atlantic Ocean for various meteorological conditions. The data covers a three-month period, June through August, during which different aerosol types are predominant in specific regions. Our approach eliminates outliers; sorts the data into aerosol bins; and the mean Aerosol Optical Depth (AOD) value for each bin and the corresponding mean Cloud Water Path (CWP) value are determined. The mean CWP is plotted against the mean AOD. The response curve for all aerosol types shows a peak CWP value corresponding to an aerosol loading value AOD_{peak}. The peak is used to divide the total range of aerosol loading into two sub ranges. For AOD value below AOD_{peak}, mean CWP and mean AOD are positively correlated. The correlation between mean CWP and mean AOD is negative for aerosol loading above AOD_{peak}. Irrespective of aerosol type,

atmospheric water vapor content and lower tropospheric static stability, the peak observed for each aerosol type seems to describe a universal feature that calls for further investigation. It has been observed for a variety of geographical locations and different seasons.

Keywords: cloud water path (CWP); aerosol optical depth (AOD); correlation

List of Symbols

AOD	Aerosol Optical Depth
LTSS	Lower Tropospheric Static Stability
WV	Water Vapor
CWP	Cloud Water Path
AAI	Absorbing Aerosol Index
NAADR_Marine	Non Absorbing Aerosol Dominated Region in the marine environment. This aerosol type has a strong sea salt component.
NAADR_Land	Non Absorbing Aerosol Dominated Region over land. This aerosol type has a strong sulfates component.
AADR_Sahara	Absorbing Aerosol Dominated Region in the Sahara environment. This aerosol type has a strong dust component.
AADR_Urban	Absorbing Aerosol Dominated Region in urban environment. This aerosol type has a strong soot component.
AADR_SubTrop	Absorbing Aerosol Dominated Region in Subtropical African biomass burning region. This aerosol type has a strong smoke component

1. Introduction

In the context of global climate change, aerosol and cloud interactions remain the most uncertain factor because the mechanisms that link aerosol to cloud properties change are carried out through processes that are not well understood [1]. Investigations involving cloud and aerosol showed positive, negative or no correlation between aerosol and cloud properties in general and cloud water path particularly. The Advanced Very High Resolution Spectro-Radiometer (AVHRR) retrieved cloud and aerosol properties showed a negative correlation between the column cloud condensation nuclei (CCN) concentration and the effective radius and a positive correlation with cloud liquid water path over the ocean [2]. The POLarization and Directionality of the Earth's Reflectance (POLDER) instrument retrieved cloud and aerosol properties that showed a negative correlation exists over both land and ocean [3]. The AVHRR water path and the column CCN were found not only positively correlated [4] but also negatively correlated on the global scale [5]. It has been suggested that the correlation between these parameters may be positive or negative and vary regionally [6], while the results of a study conducted by Kaufman in 2005 suggested that the sign of the correlation may depend on aerosol type [7]. One of the most significant consequences of the observed divergences in correlative studies was the intense search for possible physical mechanisms or factors that could explain the disparities in the results between scientists.

1.1. Suggested Mechanisms Leading a Positive Correlation

The mechanisms likely to result in increased in cloud liquid water as aerosol loading increases are associated with precipitation.

a. Aerosol affects clouds: The addition of aerosol causes a decrease in drop size, precipitation is suppressed, and clouds develop further before raining out (if they ever do) and last longer in the more developed stage, thus increasing average Cloud Water Path (CWP) [8,9].

b. Clouds affect aerosol: Following a precipitation event the aerosol loading is dramatically reduced, as is the cloud development (the clouds "rain out"). Low aerosol is thus associated with low CWP [10].

1.2. Suggested Mechanisms Leading a Negative Correlation

Several mechanisms would cause cloud development to decrease as aerosol loading increases.

a. Aerosol affects clouds: (Surface shading) Aerosols shade the surface, reducing surface heating and evapotranspiration so that cloud liquid water is reduced [11].

b. Aerosol affects clouds: (Atmospheric heating) Absorbing aerosols (such as smoke or dust) can heat the upper levels of the troposphere, which in combination with surface shading stabilizes the atmospheric column and reduces cloud development [11–14].

c. **Aerosol affects clouds:** (Clouds drop size) As an increase in CCN leads to smaller droplets, evaporation around the sides and top of clouds due to mixing will become more effective at reducing the cloud liquid water [11,15].

d. **Aerosol and meteorology affect clouds:** High-pressure systems inhibit convective activity, simultaneously reducing cloudiness while not allowing smoke (other aerosols with sources in the region) to "vent" away from the source region [16].

e. Clouds and meteorology affect aerosol: In a humid environment and in areas surrounding clouds, significant aerosol hygroscopic growth has been observed [17].

1.3. Other Factors

Many studies pointed out the methodological differences in assessing the effects of aerosol on CWP as possible source for divergence.

a. Bulk scheme simulation *vs.* Bins microphysics scheme simulation [18,19].

b. CWP averaging method over the domain: full grid points averaging *vs.* conditional (cloud only) grid points averaging [20].

c. Cloud regimes: Stratocumulus *vs.* Trade wind cumulus [21].

d. Analysis scales *vs.* Process scales [22].

Exploring alternative explanations to understand the disparity between studies is the motivation behind this study. Here, we focus on the statistical method used to trace the relationship between observational aerosol and cloud proxies, which, to our knowledge, has not been questioned in these past studies. Correlations in many studies have been established by linearly regressing aerosol proxies against cloud properties (as indicated in Figure 1). An example of this approach could be found in [23].

However, the results of statistics applied to a dataset and the inferred interpretations could vary greatly from one range of the dataset to another. In the context of cloud and aerosol interaction, modeling studies in a controlled environment can discretely increase aerosol loading and for each aerosol loading determine precisely the modeled the response of cloud proxies. The results of these modeling studies have shown a strong correlation between aerosol loading range and the response of cloud water path [24,25]. Unlike modeling studies, observational studies rely on snapshots of the atmospheric scenes produced by satellites to infer correlations between aerosols optical depth and cloud water path, requiring assumptions about the cloud lifecycle to relate correlations to physical mechanisms [6,10,26]. In addition, many observational studies in the past did not consider the effects of varying Aerosol Optical Depth (AOD) ranges in their statistical analysis in order to determine the correlation between CWP and AOD. In Figure 2 for example, the mean CWP response to the mean AOD varies in terms of mean AOD ranges. Which correlation describes best the relationship between aerosol and cloud proxies in the dataset?

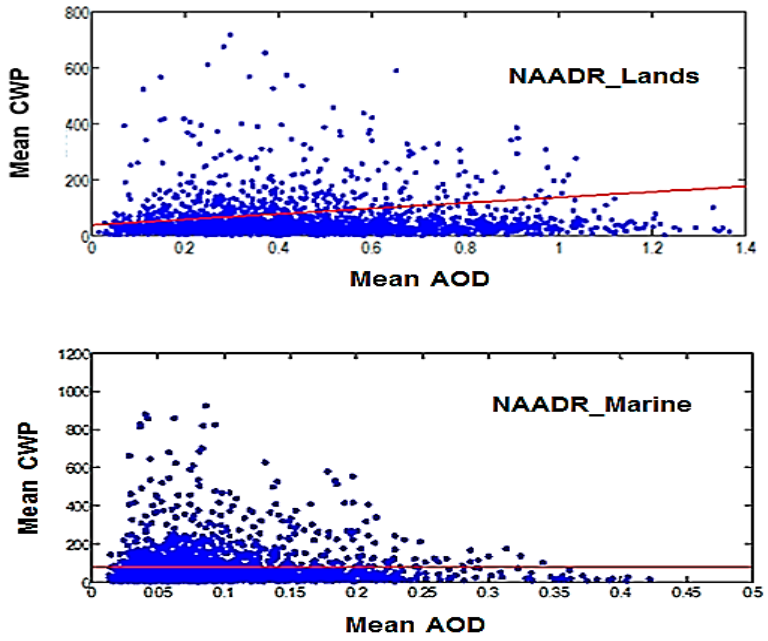

Figure 1. Shows for both NAADR_Land (sulfate) and NAADR_Marine (sea salt), respectively, a positive and a negative correlations by single line linear regression method between mean cloud water path (CWP) and mean aerosol optical depth (AOD) over the total AOD range, for non-binned aerosol data and outliers not removed. In contrast to techniques presented later, there is no averaging or removal of outliers.

The methodology we propose characterizes the response of cloud water path in terms of aerosol loading ranges for satellite data. Our results could shed some light on a possible source of the disparities in observation based past correlative studies.

This paper is organized around six major Sections. Section 1 presents the context of this work. Section 2 describes both the study areas where investigations were conducted as well as the data used. The steps of the analytical method and the partial results when the method is applied to NAADR_Marine and NAADR_Land are described in Section 3. Section 4 evaluates the effects of

meteorology on CWP response to increasing AOD by both statistic compositing and multilinear regression analysis. Section 5 contains the discussion part of the paper. In this Section, a parallel is established between the single line linear regression method (Figure 1) and our approach in order to reveal a potential source of divergence in past correlative studies. Finally Section 6 concludes the paper by summarizing the main points we attempted to make.

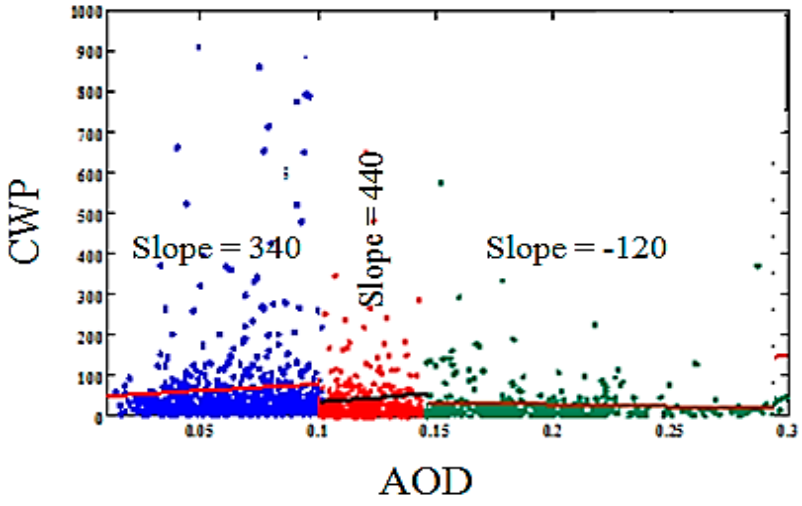

Figure 2. Correlations between aerosol optical depth (AOD) and cloud water path (CWP) in southern region of Africa for three different ranges of AOD from the same dataset. The low ranges of AOD (0; 0.1) (blue data points) and (0.1; 0.15) (red data points) show a positive correlation between AOD and CWP. The highest range of AOD (0.15; 0.3) (green data points) shows a negative correlation between AOD and CWP for (0.15; 0.3). The ranges were obtained by gradually increasing by 0.05 (arbitrary constant) AOD loading in the scatter plot CWP *vs.* AOD until a significant change (magnitude or sign) in the slope of the regression line occurs.

2. Study Area and Satellite Data

2.1. Study Area

During June through August, the Atlantic Ocean is covered by varying concentrations of several aerosol types, with each type dominant in a distinct latitude belt [7] as indicated in Figure 3. The regions of interest are identified by either absorbing or non-absorbing aerosol type. Sampled in Northern Atlantic (30°N–60°N), study region (**B**) is impacted by anthropogenic pollution aerosol (Sulfate) from North America and Europe. Study Area (**A**) is sampled in the Southern Tropical Atlantic (30°S–20°S) which is under strong influence of clean maritime air (Sea salt) [7]. The areas **(C)** and **(D)** are dominated by absorbing aerosol types as they are, respectively, sampled from Sahara dust and Sub-Tropical biomass burning African regions. Study region **(E)** is sampled in an area of high urban impact and is absorbing aerosol type dominated (Soot). A study area located over ocean and dominated by absorbing aerosol will be marked as AADR_Marine ("Absorbing Aerosol Dominated Region") and non-absorbing aerosol, will be marked as NAADR_Marine ("Non Absorbing Aerosol Dominated Region"). For study areas, respectively, sampled in the Sahara dust and Sub-Tropical

smoky background environments, the regions are marked as AADR_Sahara (**C**) and AADR_SubTrop (**D**). In addition, summertime in the Northern Hemisphere corresponds to wintertime in Southern Hemisphere. Study periods for E, B and C in the Northern Hemisphere covered June through August (summer) for A and D this will correspond to wintertime in the Southern Hemisphere.

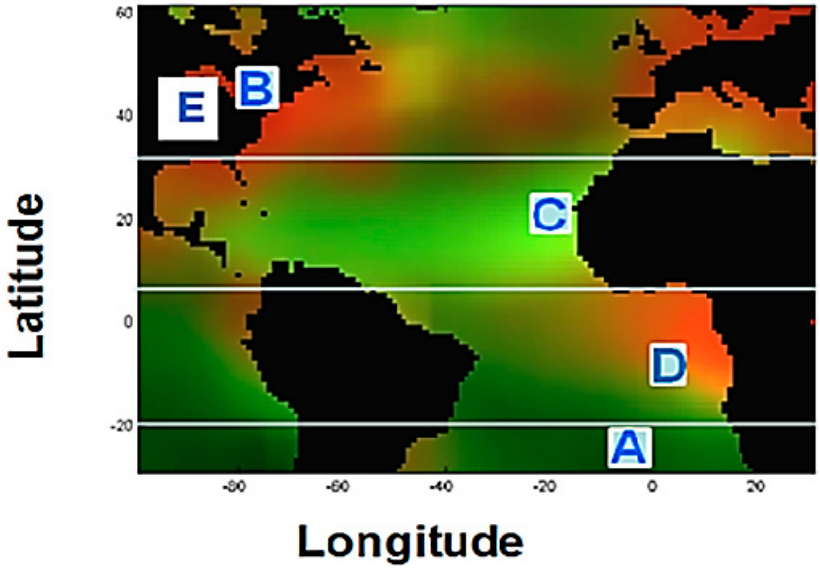

Figure 3. Shows the latitudinal distribution of study areas. Regions (**A**)–(**E**) are, respectively, characterized by as NAADR_Marine, NAADR_Land, AADR_Sahara, AADR_SubTrop, and AADR_Urban.

2.2. Satellite Data

The data used is MODIS joint atmospheric product level 2 retrieved from June through August 2005 between 14:00 and 22:00 GMT on board of Aqua platform. The day time Aqua overpass (13:30) coverage is chosen because clouds are more likely to develop in the afternoon than in the morning [26]. Once retrieved, the data was processed to meet the conditions of this study; we want to study aerosol and cloud interaction from a liquid cumulus clouds perspective because retrieval errors are smaller in the pure liquid phase, and spaces between cumulus clouds allow retrieval of aerosol nearby. The cloud top temperature (CTT) and cloud fraction (CF) were, respectively, maintained above 265 °K and less than 0.6 to capture pixels of warm, liquid cumulus clouds. The highest data density was produced by solar zenith angles between 30 and 70 degrees and view angles less than 60 degrees. The data was filtered according to these restricted angular ranges in order to minimize the influence of biases due to three-dimensional effects [10].

3. Method

Examples of the analytical method are presented using two study areas NAADR_Land and NAADR_Marine. Responses of CWP to aerosol induced perturbation for the remaining study areas are displayed with the two initial study areas in Section 3 to exhibit the general nature of the results.

3.1. Mathematical Relationships and Definition

(a) Liquid Water Sensitivity (δ)

The concepts of liquid water sensitivity and relative liquid water sensitivity were used by Han *et al.* [6] and we use the same definition with a single change in variable to assess the response of cloud water path to aerosol induced perturbation. Liquid water sensitivity as defined in Equation (3) represents the change of liquid water path *vs.* column droplet number concentration (a proxy for aerosol particle count), which is affected by the total water availability [6]. The sensitivity is denoted by δ, and is derived using the least-squares linear regression to determine the slope of ΔLWP (change in cloud liquid water path) and ΔN_c (change in droplets number concentration). This formulation of δ assesses the response of cloud water path response to cloud condensation nuclei independently of the actual aerosol type retrieved. This was intentional to eliminate dependence on aerosol type.

The two variables used to compute δ, are derived from both cloud drop effective radius (r_e) and cloud optical depth(τ). The droplet number of concentration N_c is defined as function of CWP [27] and represented by Equation (1).

$$N_c = \frac{3}{4\pi\rho_w} \cdot \frac{\mathrm{CWP}}{r_e^3(1-b)(1-2b)} \tag{1}$$

where r_e is the cloud drop effective radius and b is effective variance of cloud droplet size distribution. CWP is calculated using both τ and r_e [28] as indicated in Equation (2).

$$\mathrm{CWP} = \frac{2}{3} r_e \tau \rho_w \tag{2}$$

where τ is the cloud optical depth.

From these two definitions, δ is derived [6] as indicated in Equation (3).

$$\delta = \frac{\Delta \mathrm{CWP}}{\Delta N_c} \tag{3}$$

(b) Liquid Water Relative Sensitivity β

When the liquid water sensitivity is normalized for different environments, it isolates better the effect of aerosol-cloud interaction [6]. Cloud water path relative sensitivity is defined as in Equation (4).

$$\beta = \frac{\Delta \mathrm{CWP} / \mathrm{CWP}}{\Delta N_c / N_c} \approx \frac{\Delta \ln(\mathrm{CWP})}{\Delta \ln(N_c)} \tag{4}$$

Approximating the droplet number of concentration (sometimes referred to as aerosol loading in this study) to aerosol optical depth [29], we define the relative sensitivity β in terms of CWP and AOD in our study. β is then used to statistically trace aerosol-cloud relationship. This approximation is based on the assumption that moisture is uniformly distributed in the cloudy atmosphere. In that instance, aerosol swelling in humid environment could be interpreted as an increase in aerosol loading [17]. Increase in aerosol loading produces numerous but smaller cloud droplets [30,31]. The presence of ratio in the formula of the relative sensitivity compensates for possible variations in the proportionality

factor between N_c and AOD, and similar variations in retrievals of CWP. This makes β a suitable parameter to assess the correlation between CWP and AOD. We assumed $N_c = k \times$ AOD where k is a constant, then k will cancel out in Equation (4), so that our form of beta expressed in terms of CWP and AOD and represented by Equation (5) is the same as in Equation (4).

$$\delta = {\Delta \mathrm{CWP}}/{\Delta \mathrm{AOD}}$$

$$\beta = {\Delta Log[\mathrm{CWP}]}/{\Delta Log[\mathrm{AOD}]} \quad (5)$$

β sometime has been known in literature as λ and is believed to be difficult to measure because of rapid adjustment of CWP to aerosol-induced perturbation [20].

Much of the effect on CWP is due to rainfall, as seen by both modeling [32,33] and observations [34] studies. The picture remains unclear with variability of the results in the literature attributed to averaging scale [35], phases of cloud life cycle [35,36] and aerosol loading [36]. Given these factors plus the relative sparseness of retrieved rainfall over the ocean sites in this study, we chose to leave rainfall as a hidden variable in this study.

The goal here is not so much to accurately quantify β, but to assess its variability. We will demonstrate the non-monotonic behavior of the CWP response to increasing AOD by computing and comparing the slopes of CWP *vs.* AOD, log(CWP) *vs.* log(AOD) and the corresponding correlation coefficients during "moistening" and "drying" (these terms are clearly defined in Section 3 for different types of aerosol when: (1) the data is not binned and outliers are not removed; and (2) the data is averaged by bins and outliers are removed).

In addition to aerosol, cloud formation involves both the dynamics of convection and moisture availability. We anticipate the sensitivity of CWP response to atmospheric static stability as well the atmospheric content of precipitable water vapor as meteorological parameters. CWP response for each type of aerosol is determined for low and high Water Vapor (WV) environment as well as low and high lower tropospheric static stability (LTSS) environment in order to assess the influence of meteorology. Moreover, to determine which variables (aerosol or meteorology) is the governing variable of CWP response (increase/decrease during Moistening/Drying), CWP and all the meteorological parameters are binned, respectively, in AOD moistening and drying ranges and coupled with multilinear regression analysis in each case.

3.2. Data Preparation (*Elimination of Outliers/Bins Averaging*)

Outliers may occur in cloud and aerosol data for many reasons. Cloud contamination may affect aerosol data [7]. Sources of cloud contamination include:

1. High concentration of broken clouds that may induce illumination of aerosol field beyond 500-m distance from the clouds [37].
2. Relative humidity can affect both aerosol and cloud amount and may result in a change of the ratio of aerosol optical depth to cloud condensation nuclei through aerosol swelling [38].

This Section will be illustrated using two study areas. NAADR_Land located in Northern hemisphere and NAADR_Marine located in Southern Hemisphere. We will only show the results for

the remaining study areas. Least squares regressions are strongly influenced by outliers. In order to avoid skewed correlations between CWP and AOD, we used the data smoothing technique according to Eilers *et al.*, [39] where outliers are defined as points regions where data density is less than a fraction of the maximum density. The minimum threshold density to deciding which data points to be considered for this study was set at 50, approximately 20% of the maximum density. We carefully select a box avoiding outliers (white dots) containing data points density layers ranging from 50 to 250 to define our working data ranges; the corresponding data ranges were: AOD (0.05–0.60), (0.01–0.20), respectively, for region **B** and for region **A**. CWP (0–200 g/m^2) for both regions (see Figure 4). Many other boxes with data point's density ranges and defining various AOD and CWP ranges can be drawn; our choice maximized the dataset size by eye.

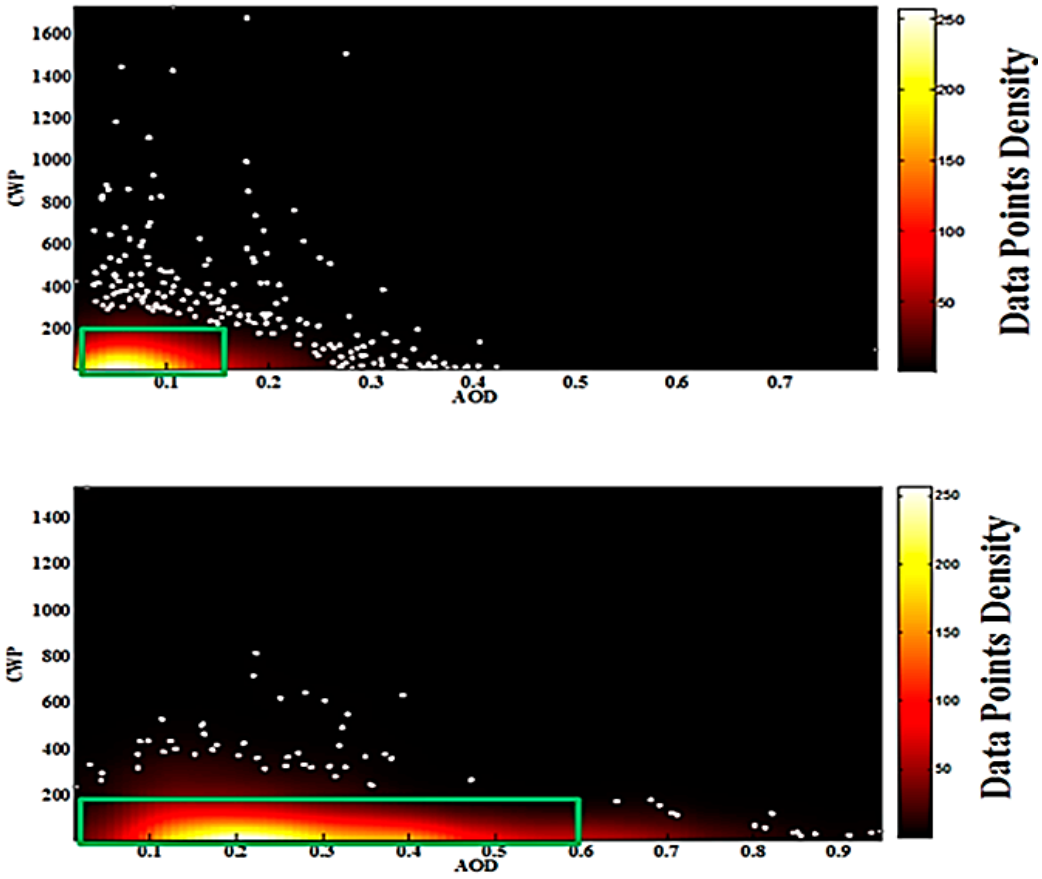

Figure 4. Data points' density distribution in a cloud water path (CWP) *vs.* aerosol optical depth (AOD) plot for NAADR_Marine (**Top**) and NAADR_Land (**Bottom**). The green rectangle indicates the best ranges of AOD and CWP to obtain a minimum of 50 data points density per AOD bin (0.01) and (0.05), respectively, for NAADR_Marine and NAADR_Land. The range for AOD are [0, 0.15] & [0, 0.6] and CWP [0; 200].

To demonstrate the non-monotonic behavior of CWP response, we divide the full range of AOD into bin sizes of 0.05 (NAADR_Land) and 0.01 (NAADR_Marine). The characteristics mean AOD and mean CWP per data points in each bin were calculated and Mean AOD is plotted against mean CWP (Figure 5).

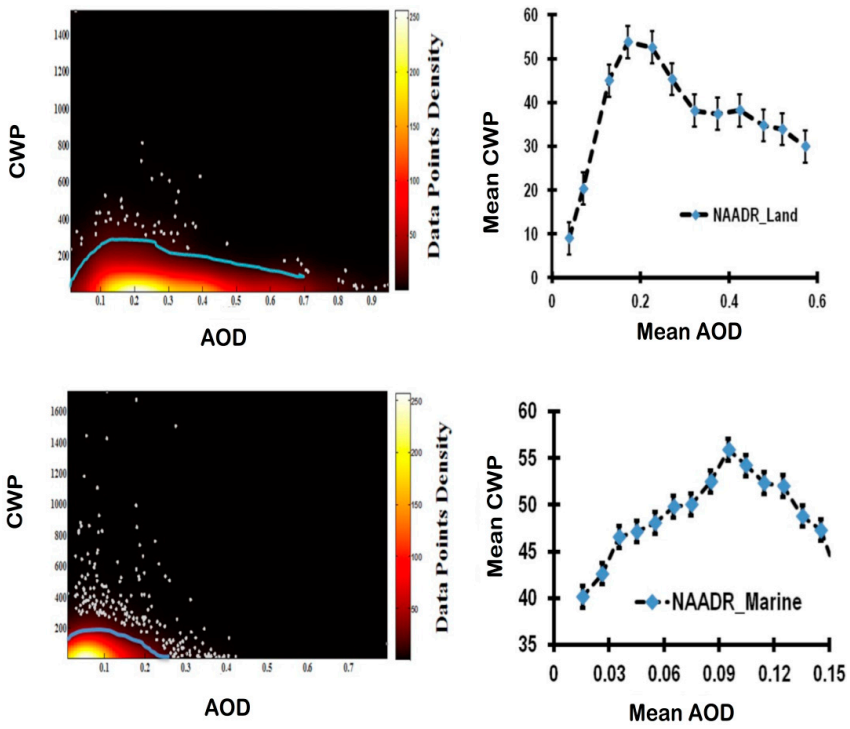

Figure 5. (**Top**) Shows for NAADR_Land the average behavior of cloud water path (CWP) to increasing aerosol optical depth (AOD) for all data density layers excluding outliers (White dots) (**Left**) and the plot of CWP *vs.* AOD after binning (**Right**). Each bin will have both an average and a standard deviation (**Bottom**) Shows for NAADR_Marine the average behavior of CWP to increasing AOD for all data density layers excluding outliers (White dots) (left) and the plot of CWP *vs.* AOD after binning (right).

3.3. Description of Cloud Water Path (*CWP*) *Response to Increasing Aerosol Optical Depth* (*AOD*)

When AOD mean is plotted against mean CWP, a peak is observed in both graphs. This peak is used to divide the full data range into two sub ranges. As aerosol loading increases, the graphs show an initial increase in CWP to the peak followed by a decrease for all five regions (see Figure 6). For simplification purposes and to indicate the occurrence of two distinct and opposite behaviors, the initial increase in CWP to maximum (CWP_{peak}) that occurs as aerosol loading increases is referred to as "moistening" and the decrease in CWP from CWP_{peak} that occurs as aerosol loading increases from AOD_{peak} to higher aerosol loading is referred to as "drying". "Moistening" and "drying" are descriptive of the shape of the response curves only, and are not meant to represent any physical processes that are actually occurring in these ranges (see Figure 7). The relative sensitivity of CWP to AOD β is calculated as the slope of the plot log (mean CWP) *vs.* log (mean AOD) for each sub-range. The magnitudes and the signs of β (see Table 1) show a non-monotonic response of cloud water path to increasing aerosol loading contrary to a monotonic response suggested when Single Line Linear Regression method was applied to the same datasets. The correlation coefficients for both binned non-logarithmic and binned logarithmic data in the two regions are significantly high compared to the correlation coefficients determined before the data is binned and the outliers are removed. A large part of the increase in correlation coefficients is due to averaging, but also to the excluded outliers' contributions.

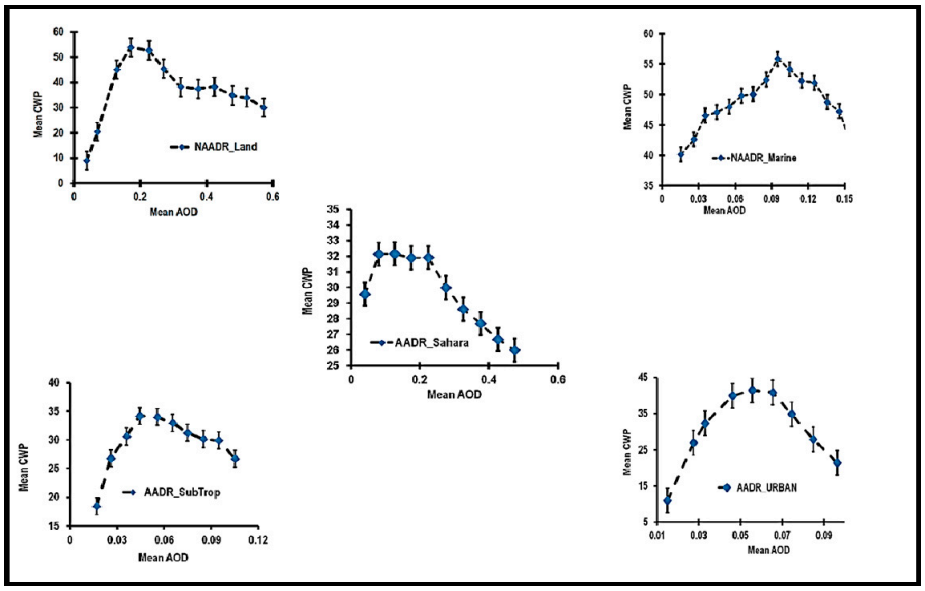

Figure 6. Responses of cloud water path (CWP) to increasing aerosol optical depth (AOD) for all five study regions. CWP initially increases to a maximum followed by a decrease in each case. CWP sensitivities during moistening and drying are calculated from the response curves as the slopes of mean CWP *vs.* mean AOD during both moistening and drying. For each average point shown above, the standard deviation is shown as error bars.

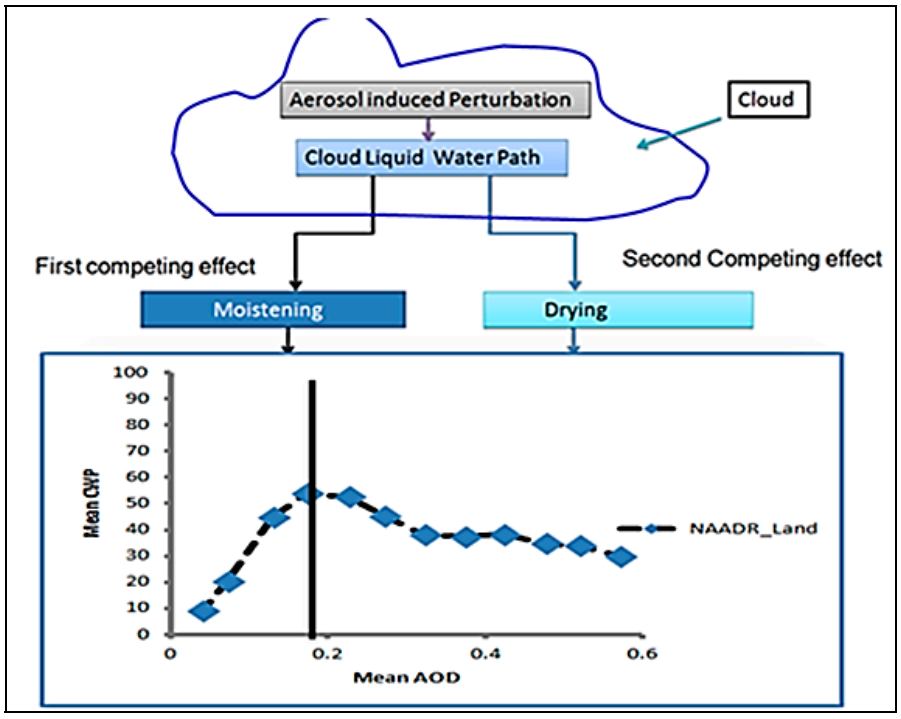

Figure 7. Illustration of cloud and aerosol interaction that resulted in an initial increase (moistening) of cloud water path (CWP) to a maximum followed by a decrease (drying) as aerosol optical depth (AOD) increases for NAADR_Land.

Table 1. Correlation coefficients (R^2), sensitivity (δ), relative sensitivity (β) and slope (a^*) of the regression line (before binning) of cloud water path (CWP) to increasing aerosol optical depth (AOD) as function of AOD ranges and aerosol type.

Parameters	R^2/β	R^2/δ	R^2/a^*
NAADR_Land	--	--	--
AOD Ranges	--	--	--
[0.02, 0.172]	0.991/1.22 ± 1.69	0.984/348.3 ± 1.74	0.183/180 ± 0.226
[0.172, 0.6]	0.916/−0.514 ± 1.69	0.844/−53.54 ± 1.74	0.05/−160 ± 0.226
NAADR_Marine	--	--	--
AOD Ranges	--	--	--
[0, 0.095]	0.950/0.16 ± 0.27	0.950/171.7 ± 1.88	0.003/130 ± 0.271
[0.095, 0.15]	0.860/−0.58 ± 0.27	0.911/−221 ± 1.88	0.0004/−270 ± 0.271

* Slope is computed before outliers are removed and the data is sorted into aerosol optical depth bins.

4. Effects of Varying Meteorological Parameters on Cloud Water Path (CWP) Response to Increasing Aerosol Optical Depth (AOD)

Although it is tempting to speculate on the physical mechanisms behind the observations produced by these two methods, the context in which the interactions occur between variables is too complex to be completely explored by the current dataset, so we prefer to leave such discussion to future investigations. The reader is referred to the many possible mechanisms described in the introduction.

4.1. Evaluation by Atmospheric Water Vapor (WV) Statistical Compositing

The responses of CWP to increasing AOD are evaluated in high and low atmospheric water vapor content environment for the five study areas. WV path was used as a direct satellite measurement. The total WV range for each study area is divided into two subranges of nearly equal counts based on WV histogram data distribution. Low WV range is low WV relative to high WV (High WV range).

The characteristics parameters of CWP response curves are determined in each case and tabulated for comparison purpose.

4.1.1. NAADR_Marine

In Figure 8, the threshold aerosol loading necessary to shift from cloud moistening process to drying process is larger in high water vapor environment than in low water vapor environment as well as the corresponding cloud water paths.

In Table 2, the transition from low to high water vapor regime resulted in a significant increase (↑) in keys parameters (AOD_{peak}, CWP_{peak}, $\beta_{moistening}$, β_{drying}) of cloud water path response curve to aerosol induced perturbation. β_{drying} increases nearly 10 times from a low to high water vapor regime and this is also the most significant magnitude change. The lowest magnitude change occurred in $\beta_{moistening}$ (29%).

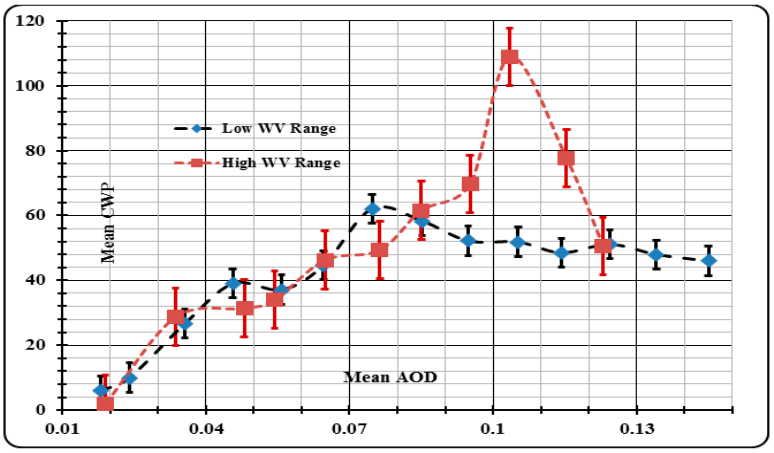

Figure 8. Response of cloud water path (CWP) to increasing aerosol optical depth (AOD) in low and high atmospheric WV environments for NAADR_Marine.

Table 2. Comparative table of the percent increase (↑) in the characteristics parameters of cloud water path response curve to aerosol induced perturbation from low to high water vapor environment for NAADR_Marine.

Moisture	AOD_{peak}	CWP_{peak}	$\beta_{moistening}$	β_{drying}
Low WV	0.074 ± 0.011	62.13 ± 1.74	1.59 ± 0.17	–0.417 ± 0.17
High WV	0.104 ± 0.011	109 ± 1.74	2.050 ± 0.20	–4.319 ± 0.20
($\Delta X/X$ Low WV) %	40.5% ↑	75.4% ↑	29% ↑	936% ↑

4.1.2. NAADR_Lands

The threshold aerosol loading necessary to shift from cloud moistening process to drying process is much larger in low water vapor environments than in high water vapor environments as well as the corresponding cloud water paths (Figure 9). The availability of moisture in high WV environments could offset the drying effect induced by increasing aerosol loading compared to CWP response in low water vapor environments. In Table 3, except for $\beta_{moistening}$, all characteristic parameters AOD_{peak}, CWP_{peak}, β_{drying} for NAADR_ Land decreased significantly from low to high water vapor environments In high WV vapor environments, $\beta_{moistening}$ exhibits the highest magnitude compared to β_{drying} (moistening is the highest sensitivity mechanism) while drying the is the highest sensitivity mechanism in low WV conditions. During the transition from low to high atmospheric water vapor content, the most significant magnitude change occurred in $\beta_{moistening}$ (143% increase) while the lowest magnitude change occurred in CWP_{peak} (11% decrease).

Table 3. Comparison of percent increase (↑) or decrease (↓) in the characteristics parameters of cloud water path response curve aerosol induced perturbation from low to high water vapor environment NAADR_Land.

Moisture	AOD_{peak}	CWP_{peak}	$\beta_{moistening}$	β_{drying}
Low WV	0.419 ± 0.036	77.40 ± 2.84	0.212 ± 0.06	–0.492 ± 0.180
High WV	0.275 ± 0.036	69.11 ± 2.84	0.515 ± 0.06	–0.217 ± 0.01
($\Delta X/X$ Low WV) %	34% ↓	11% ↓	143% ↑	56% ↓

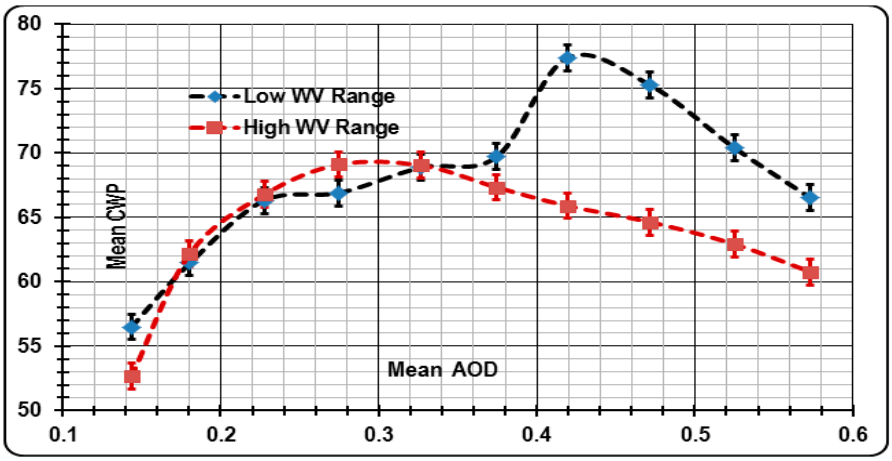

Figure 9. Response of cloud water path (CWP) to increasing aerosol optical depth (AOD) in low and high atmospheric WV environments for NAADR_Land.

4.1.3. AADR_Urban

For AADR in urban area (Figure 10), the threshold aerosol loading to shift from low to high water vapor environments is increased by approximately 3.2%. Meanwhile the corresponding CWP decreased significantly. In Table 4, CWP_{peak}, β_{drying} and $\beta_{moistening}$ decrease from low to high WV environments, respectively, by 20.2%, 82.2% and 36.1% of their initial magnitudes. Drying is the highest sensitivity process (highest β magnitudes) in both high and low water vapor environments.

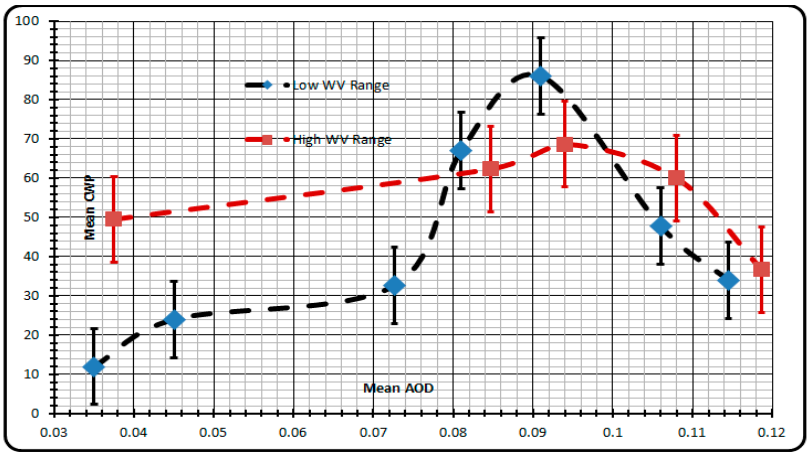

Figure 10. Response of cloud water path (CWP) to increasing aerosol optical depth (AOD) in low and high atmospheric water vapor (WV) environments for AADR_Urban.

Table 4. Comparative table of percent increase (↑) or decrease (↓) in the characteristics parameters of cloud water path response curve aerosol induced perturbation from low to high water vapor environment AADR_Urban.

Moisture	AOD_{peak}	CWP_{peak}	$\beta_{moistening}$	β_{drying}
Low WV	0.091 ± 0.031	86.0 ± 2.46	1.846 ± 0.180	–4.014 ± 0.180
High WV	0.094 ± 0.031	68.67 ± 2.46	0.328 ± 0.122	–2.563 ± 0.122
($\Delta X/X$ Low WV) %	3.2% ↑	20.2% ↓	82.2% ↓	36.1% ↓

4.1.4. AADR_SubTrop (Southern Africa)

In Figure 11, mean CWP increases with increasing mean AOD up to 0.095 and 0.084 (mean AOD values) for, respectively, low and high water vapor environments. In Table 5, Drying is the highest sensitivity mechanism in both low and high water vapor environment. β_{drying} magnitude is reduced by nearly 23% from low to high water vapor environment while $\beta_{moistening}$ is increased by 132%. The threshold aerosol loading necessary to shift from moistening to drying is decreased by approximately 13% from high to low water vapor environment.

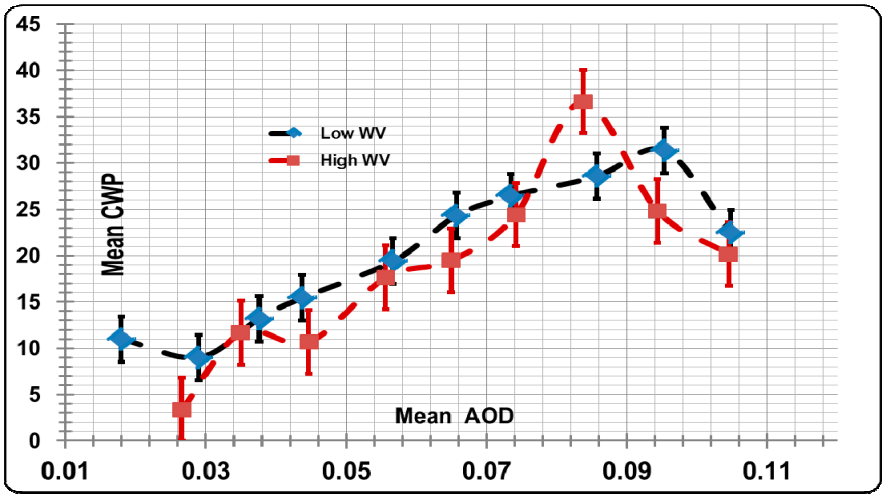

Figure 11. Response of cloud water path (CWP) to increasing aerosol optical depth (AOD) in low and high atmospheric water vapor (WV) environments for AADR_SubTrop.

Table 5. Percent increase (↑) or decrease (↓) in the characteristic parameters of cloud water path (CWP) response curve to increasing aerosol optical depth (AOD) for low and high atmospheric water vapor (WV) environments for AADR_SubTrop. The maximum and minimum changes are, respectively, observed for $\beta_{moistening}$ and AOD_{peak}.

Moisture	AOD_{peak}	CWP_{peak}	$\beta_{moistening}$	β_{drying}
Low WV	0.095 ± 0.028	31.35 ± 2.20	0.731 ± 0.238	–3.512 ± 0.238
High WV	0.084 ± 0.028	36.60 ± 2.20	1.693 ± 0.173	–2.719 ± 0.173
($\Delta X/X$ Low WV) %	13.1% ↓	16.7% ↑	131.6% ↑	22.6% ↓

4.1.5. AADR_Sahara

In Figure 12, CWP responses to AOD induced perturbation in high and low water vapor environments are nearly horizontal mirror images of each other. In Table 6, Drying and moistening are, respectively, the highest sensitivity process in low and high water vapor environments. From low to high WV environments, the maximum CWP corresponding to the lowest aerosol loading is reduced by approximately 30%.

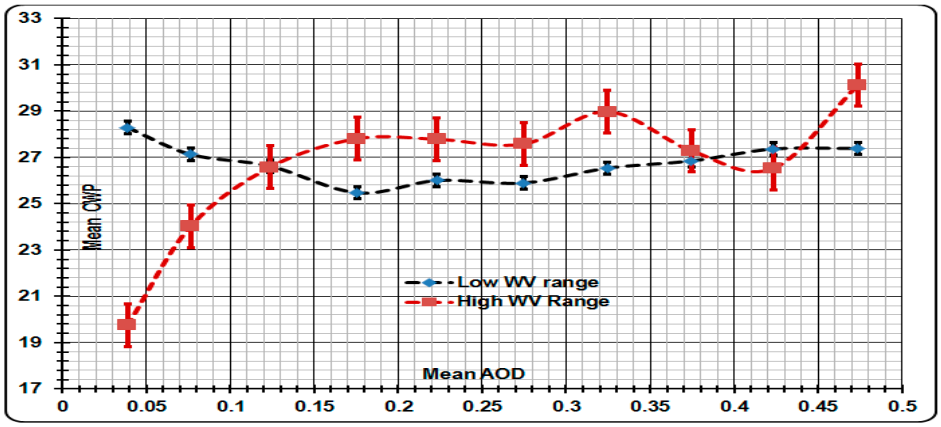

Figure 12. Response of cloud water path (CWP) to increasing aerosol optical depth (AOD) for low and high atmospheric WV environments for AADR_Sahara.

Table 6. Percent of decrease (↓) in the characteristics parameters of cloud water path response curve to aerosol induced perturbation from low to high water vapor environment AADR_Sahara Drying is the highest sensitivity mechanism in low water vapor environment while moistening is the highest sensitivity mechanism in high water environment.

Moisture	AOD_{peak}	CWP_{peak}	$\beta_{moistening}$	β_{drying}
Low WV	0.04 ± 0.004	28.3 ± 2.20	--	–0.07 ± 0.238
High WV	0.04 ± 0.031	19.75 ± 2.20	0.230 ± 0.238	--
($\Delta X/X$ Low WV) %	0% ↓	30% ↓	--	--

4.2. Evaluation by Lower Tropospheric Static Stability (LTSS) Statistical Compositing

We study the sensitivity of CWP to AOD under conditions of varying lower tropospheric static stability (LTSS), comparing moistening and drying processes. LTSS data was collected from MODIS collection 5, where LTSS data is stored under stability indices, which are taken from ECMWF or NOAA NCEP reanalysis data. The total LTSS range for each study area is divided into two subranges (Low and High LTSS) of nearly equal counts based on LTSS histogram data distribution.

4.2.1. NAADR_Marine

In Figure 13, the response of CWP to AOD is non monotonic in both stable and unstable environments; the threshold aerosol loading necessary to shift from cloud moistening process to drying process is much larger in high stability environments than in low stability environments as well as the corresponding CWP. The magnitudes of cloud liquid water sensitities δ during moistening in both stable and unstable environments are much larger than δ during drying The magnitude of $\beta_{moistening}$ is much larger in unstable environments than in stable environments. The magnitude β_{drying} is much larger in high stability environments than in low stability environments.

In Table 7, the transition from low to high static stability regime resulted in a significant increase in the parameters (AOD_{peak}, CWP_{peak}, β_{drying}) of cloud water path response curve to aerosol induced perturbation except for $\beta_{moistening}$ observed to decrease. β_{drying} increases nearly 273% from a low to high static stability regimes. The magnitude of $\beta_{moistening}$ is nearly 10 times β_{drying} in unstable atmospheric conditions.

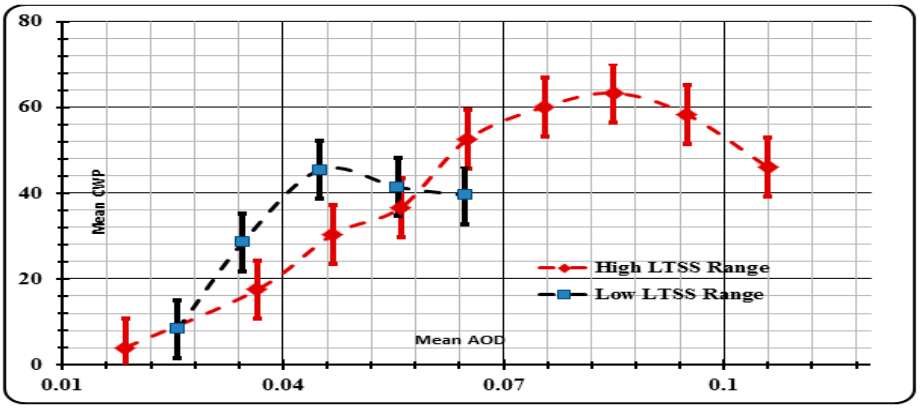

Figure 13. Response cloud water path (CWP) to increasing aerosol optical depth (AOD) in unstable and stable atmospheric environments for NAADR_Marine. The threshold AOD necessary to shift from moistening to drying processes is much larger in high LTSS environments than in low LTSS environments as well as the corresponding CWP.

Table 7. Percent of increase (↑) or decrease (↓) in the characteristics parameters of cloud water path response curve aerosol induced perturbation from low to high lower tropospheric static stability (LTSS) environments for NAADR_Marine. Except for $\beta_{moistening}$ every other parameter increased significantly from unstable to stable environments.

Stability	AOD_{peak}	CWP_{peak}	$\beta_{moistening}$	β_{drying}
Low LTSS	0.045 ± 0.011	45.42 ± 1.74	3.041 ± 0.27	–0.388 ± 0.27
High LTSS	0.085 ± 0.011	63.31 ± 1.74	1.958 ± 0.22	–1.446 ± 0.22
($\Delta X/X$ Low LTSS) %	88% ↑	39.4% ↑	35.6% ↓	273% ↑

4.2.2. NAADR_Land (Continental US)

In Table 8, except for the observed increase in AOD_{peak}, the transition from low to high static stability regime resulted in a significant decrease in the following keys parameters: CWP_{peak}, $\beta_{moistening}$, β_{drying}. The maximum decrease is observed in $\beta_{moistening}$ (89%) from low to high static stability regimes. The magnitude of $\beta_{moistening}$ in unstable atmospheric conditions is nearly five times the magnitude of β_{drying}. In stable atmospheric conditions, the magnitudes of both $\beta_{moistening}$ and β_{drying} are nearly identical. In Figure 14, for NAADR_Land, AOD_{peak} is much lower in low LTSS regimes than in high LTSS regimes.

Table 8. Percent of increase (↑) or decrease (↓) in the characteristics parameters of cloud water path response curve to aerosol induced perturbation from low to high lower tropospheric static stability (LTSS) environments for NAADR_Land. Except for AOD_{peak} observed to increase, every other parameter decreases from low to high LTSS.

Stability	AOD_{peak}	CWP_{peak}	$\beta_{moistening}$	β_{drying}
Low LTSS	0.243 ± 0.011	161 ± 1.74	11.15 ± 0.27	–2.67 ± 0.27
High LTSS	0.354 ± 0.011	70.0 ± 1.74	1.24 ± 0.22	–1.352 ± 0.22
($\Delta X/X$ Low LTSS) %	16.5% ↑	56.5% ↓	89% ↓	49.4% ↓

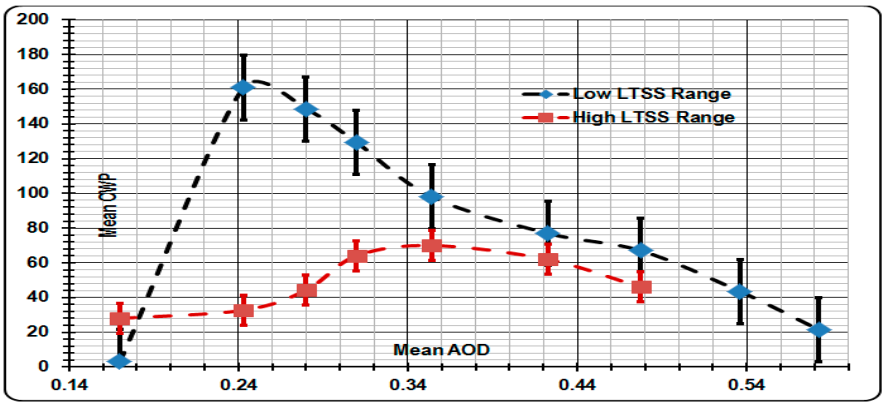

Figure 14. Response of cloud water path (CWP) to increasing aerosol optical depth (AOD) in unstable and stable atmospheric environments. For NAADR_Land, the threshold AOD necessary to shift from moistening to drying processes is much larger in stable environments.

4.2.3. AADR_Sahara

In Table 9, the magnitude of the moistening process is significantly higher than drying in high LTSS. The absence of data for low LTSS shows the prevalence of high static stability condition; this situation is consistent with the permanent high subsidence (high pressure) occurring in the Sahara region due the falling branches of Ferrell and Hadley cells. This lack of unstable conditions is reflected in Figure 15.

Table 9. Percent of increase (↑) or decrease (↓) in the characteristics parameters of cloud water path response to aerosol-induced perturbation for high lower tropospheric static stability (LTSS) environments for AADR_Sahara. No aerosol or cloud properties data were available for low static stability conditions.

Stability	AOD_{peak}	CWP_{peak}	$\beta_{moistening}$	β_{drying}
Low LTSS	--	--	--	--
High LTSS	0.221 ± 0.12	35.48 ± 1.95	0.591 ± 0.245	–0.026 ± 0.245
($\Delta X/X$ Low LTSS) %	--	--	--	--

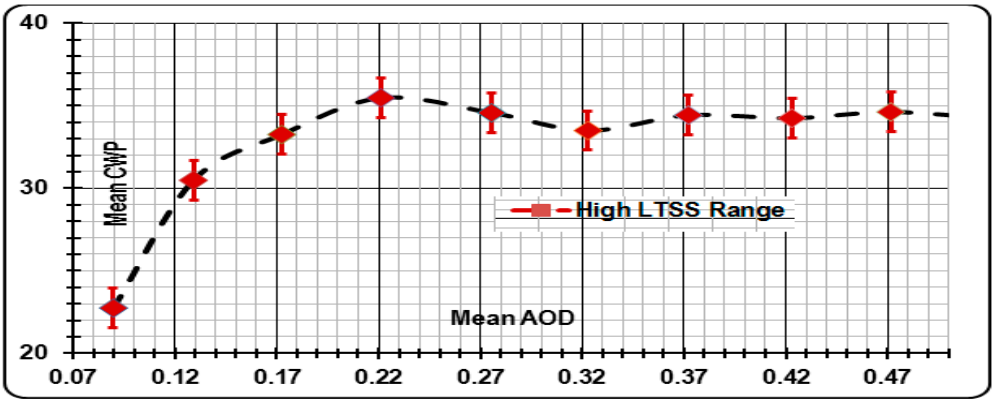

Figure 15. Response of cloud water path (CWP) to increasing aerosol optical depth (AOD) for high lower tropospheric static stability (LTSS) (stable atmospheric conditions). No data was available for low LTSS, possibly due high subsidence in the region.

4.2.4. AADR_SubTrop (off the coast of Southern African Agricultural Region).

In Figure 16, the threshold AOD necessary to shift from the moistening to drying is much larger in unstable atmospheric conditions than in stable atmospheric conditions. In Table 10, except for β_{drying} observed to increase in magnitude, the transition from low to high static stability regime resulted in a decrease in AOD_{peak}, CWP_{peak}, $\beta_{moistening}$. The increase in magnitude of β_{drying} and the decrease in magnitude of CWP_{peak} from a low to high static stability regime are very close.

Table 10. Percent of increase (↑) or decrease (↓) in the characteristics parameters of cloud water path response curve to aerosol induced perturbation from low to high lower tropospheric static stability (LTSS) environment for AADR_SubTrop. The relative sensitivities during drying in unstable and stable environment are very close while they were significantly different during moistening. All parameters are observed to decrease from an unstable to a stable environment except for β_{drying}.

Stability	AOD_{peak}	CWP_{peak}	$\beta_{moistening}$	β_{drying}
Low LTSS	0.085 ± 0.004	27.12 ± 0.51	0.186 ± 0.29	–0.311 ± 0.29
High LTSS	0.035 ± 0.004	24.76 ± 0.51	0.069 ± 0.29	–0.337 ± 0.29
($\Delta X/X$ Low LTSS) %	59% ↓	9.5% ↓	63% ↓	8.4% ↑

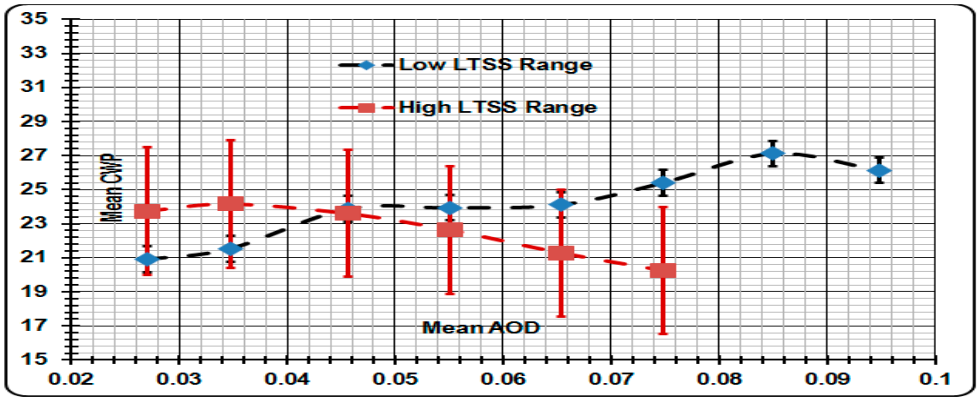

Figure 16. Response of cloud water path (CWP) to increasing aerosol optical depth (AOD) for low (unstable atmospheric condition) and high (stable atmospheric condition) lower tropospheric static stability (LTSS) for AADR_SubTrop.

4.2.5. AADR_URBAN

In Figure 17 for urban environments, moistening occurs only in unstable atmospheric condition. In stable atmospheric condition, drying is the highest sensitivity process. In Table 11, the threshold aerosol loading for AADR_Urban necessary to initiate the drying process is nearly 90% higher in low LTSS (unstable atmospheric conditions) than in high LTSS (stable atmospheric conditions). In low LTSS environment, the magnitude of relative sensitivity of CWP to aerosol induced perturbation during drying is significantly higher than its magnitude during moistening for AADR-Urban. In both Low and high LTSS environment, drying is the highest sensitivity process for AADR-Urban; no significant moistening process is occurring in high LTSS environment.

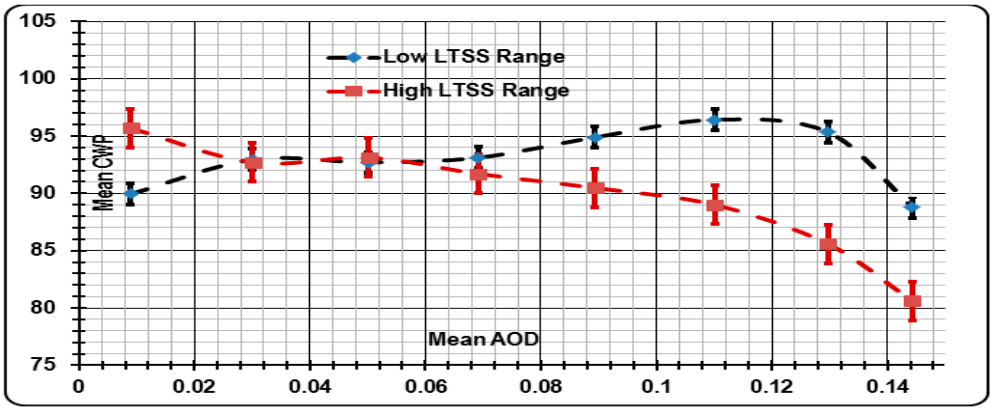

Figure 17. Response of cloud water path (CWP) to increasing aerosol optical depth (AOD) for low (unstable atmospheric condition) and high (stable atmospheric condition) lower tropospheric static stability (LTSS).

Table 11. Percent of increase (↑) or decrease (↓) in the characteristics parameters of cloud water path response curve aerosol induced perturbation from low to high lower tropospheric static stability (LTSS) environment for AADR_Urban.

Stability	AOD_{peak}	CWP_{peak}	$\beta_{moistening}$	β_{drying}
Low LTSS	0.11± 0.012	96.43 ± 1.95	0.024 ± 0.103	–0.285 ± 0.103
High LTSS	0.01 ± 0.012	95.68 ± 1.95	--	–0.047 ± 0.103
($\Delta X/X$ Low LTSS) %	91% ↓	0.7% ↓	--	83.5% ↑

4.3. Evaluation by Multilinear Regression Analysis (MLRA)

In this Section, CWP is simultaneously regressed on log (AOD), WV and LTSS. The objective of the MLRA is to untangle the influence of AOD, LTSS and WV on CWP during both moistening ($\beta > 0$) and drying ($\beta < 0$). This is done by quantifying the relative dependence of CWP on each of the three variables. Though the results generated by MLRA are known to be reliable, they still may be biased to a certain extent due to the sensitivity of MLRA to a number of factors, including:

(1) The nonlinear behavior of meteorological parameters in some regions (We suspect AADR_Sahara) may shift some meteorological influences to AOD [7].

(2) The influences of other variables unaccounted for in the context of the three variables may enhance or damp their individual influence.

(3) The direct relationship between AOD and WV observed in NAADR_Land, NAADR_Marine, AADR_SubTrop regions (Figure 18) may amplify the influence of AOD against the meteorological parameters or *vice versa*.

Though in these three regions Ridge Regression Analysis was used (a variant of the MLRA known to circumvent such situations), the possibility of error remains. Table 12 summarizes the relative influences of the three variables on CWP in the terms of regression coefficients on either side of the peak. The data is partitioned into low and high LTSS because Sections 4.1 and 4.2 showed it to have a greater effect than WV. Opposite signs in Table 12 may indicate possible antagonistic effects between

variable(s) to produce $\beta > 0$ or $\beta < 0$ in either stable or unstable atmospheric conditions, while identical sign may indicates that the variable(s) synergistically worked together to produce $\beta > 0$ or $\beta < 0$.

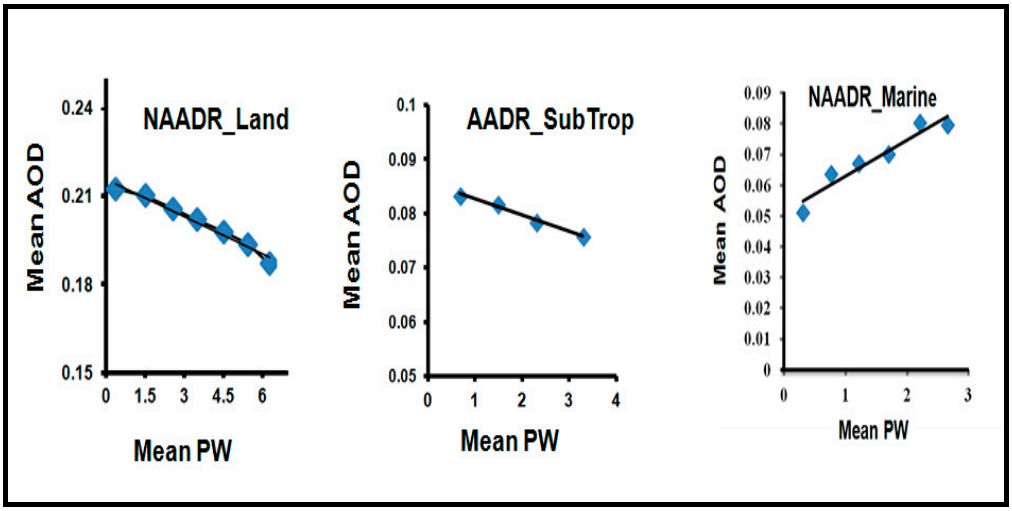

Figure 18. Linear relationship between aerosol optical depth (AOD) and Precipitable Water (PW) for NAADR_Marine, NAADR_Land and AADR_SubTrop. Ridge regression method is applicable for these three sites.

Table 12. Summary of the influences of all three variables on cloud water path (CWP) expressed as fraction the total influence (magnitudes of regression coefficients) during both moistening ($\beta > 0$) and drying ($\beta < 0$) and for each type of aerosol. Here it is assumed that the sum of the individual influence is equal to 1.

Region Type		Moistening ($\beta > 0$)			Drying ($\beta < 0$)		
		Log (AOD)	LTSS	WV	Log (AOD)	LTSS	WV
NAADR_Marine	Low LTSS	–0.52	0.39	0.09	0.33	0.50	0.17
	High LTSS	–0.52	–0.41	0.07	0.35	–0.33	–0.32
NAADR_Land	Low LTSS	0.04	0.93	–0.03	–0.05	0.92	0.03
	High LTSS	0.29	0.59	0.12	0.15	0.16	–0.69
AADR_Sahara	Low LTSS	0	–0.04	0.96	0.94	0.01	0.05
	High LTSS	0	0	–1	0.78	–0.18	–0.04
AADR_SubTrop	Low LTSS	–0.50	0.24	–0.26	0.69	0.26	0.05
	High LTSS	0.42	0.30	–0.28	0.36	–0.39	0.25
AADR_Urban	Low LTSS	0.39	0.11	0.5	0.21	0.36	0.43
	High LTSS	0.20	0.47	0.33	0.33	–0.6	–0.07

AADR_Urban:

Unstable Atmospheric Conditions (Low LTSS)

Both atmospheric AOD and WV concentrations are the governing factors that control the changes observed in CWP when $\beta > 0$. As aerosol loading increases, the strength of LTSS as controlling factor increases significantly while that of AOD and WV are observed to decrease but remain relevant. The three variables are responsible for producing $\beta < 0$.

Stable Atmospheric Conditions (High LTSS)

Atmospheric AOD , WV and LTSS are the governing factors that control the changes observed in CWP ($\beta > 0$). As aerosol loading increases ($\beta < 0$) in stable atmospheric conditions , the strength of both AOD and LTSS as controlling factor increase significantly while that of WV is observed to decrease and become irrelevant.

AADR_Sahara:

Unstable and Stable Atmospheric Conditions

Atmospheric WV and AOD are the governing factors that control changes induced in CWP.

(Respectively, $B > 0$ and $\beta < 0$). The effect of LTSS in producing either ($\beta > 0$) or ($\beta < 0$) is nearly zero, consistent with the fact that instability is not the prevailing condition in the region.

AADR_SubTrop:

Unstable and Stable Atmospheric Conditions

All three variables are governing factors in producing $\beta > 0$ or $\beta < 0$ except for WV in producing $\beta < 0$ in unstable atmospheres.

NAADR_Land:

In unstable environments, $\beta > 0$ and $\beta < 0$ processes are essentially governed by the LTSS. This is consistent with increased convective activity on land in summer. In addition, the contributions of both atmospheric WV content and AOD remain insignificant even after a substantial increase in aerosol loading. As the atmosphere becomes more and more stable, the atmospheric WV becomes the governing factors while aerosol loading as a factor gains in significance.

NAADR_Marine:

In both unstable and stable environment, $\beta > 0$ process is controlled by both LTSS and aerosol loading (AOD). The transition from an unstable environment to stable does not seem to significantly affect the impact of aerosol loading on changes that occur in CWP. In unstable and stable environment, $\beta < 0$ processes are essentially governed by all three parameters. However a significant contribution was recorded from LTSS while AOD and WV exhibited, respectively, moderate and low contributions.

5. Discussion

Observation based correlative studies in the past have exhibited contradictory results for cloud water path response to aerosol induced perturbation. In this study we have demonstrated that more attention should have been paid to how the correlations were actually established between cloud and aerosol proxies. Many past studies indirectly assumed a monotonic response of the cloud properties (CWP) to aerosol loading (AOD). The response of cloud water path to aerosol loading over the total AOD range shows an initial increase in CWP to a peak followed by a decrease over the total AOD range. This result is consistent with Xue *et al.* [40] who used Large Eddy Simulation to show an increase in CF (a proxy of CWP) to a maximum corresponding a threshold aerosol loading (100 cm^{-3}) followed by a decrease for aerosol loading greater than the threshold. Hoeve *et al.* [26] showed a peak at AOD ~0.3 in Modis COD (proxy for CWP) response to increasing AOD in Amazon biomass burning season.

Such response curves suggest that the same dataset could generate two or more different correlations between cloud variable (CWP) and aerosol loading proxies (AOD) depending on the AOD ranges the study is focused on. In that instance, there is a strong possibility that initially the divergences observed in some of the past correlative studies might have been simply an issue of analytical method [41,42].

One the advantages of this approach is that it offers the possibility to tune in meteorological parameters with cloud and aerosol proxies, determine the response curve for each meteorological setting and assess the variability in the shapes in terms of aerosol loading.

6. Conclusion

Modis aerosol and cloud observational data along with a proposed analytical method were used in this study to show the potential source of divergence in observation based past correlative studies. CWP response to increasing AOD is non monotonic and shows an initial increase to a maximum (peak) followed by a decrease. This feature persists over a range of meteorological conditions, and a variety of geographical locations and seasons. We advocate searching for a peak in the AOD-CWP curve, and confining any statistical analysis to data ranges on either side of this peak.

Acknowledgments

Data supporting this paper is Aqua Joint atmospheric product level 2 of MODIS collection 5. The data is available on MODIS website-NASA.

Author Contributions

Brian Vant-Hull had the original idea for the study, and Ousmane Sy Savane with all co-authors carried out the design. Ousmane Sy Savane was responsible for data cleaning and carried out the analyses. Ousmane Sy Savane drafted the manuscript, which was revised by all authors. All authors read and approved the final manuscript.

Conflicts of Interest

The authors declare no conflict of interest.

References

1. Lebsock, M.D.; Stephens, G.L.; Kummerow, C. Multisensor satellite observations of aerosol effects on warm clouds. *J. Geophys. Res.* **2008**, doi:10.1029/2008JD009876.
2. Nakajima, T.; Higurashi, A.; Kawamoto, K.; Penner, J.E. A possible correlation between satellite-derived cloud and aerosol microphysical parameters. *Geophys. Res. Lett*. **2001**, *28*, 1171–1174.
3. Bréon, F.M.; Tanre, D.; Generoso, S. Aerosol effect on cloud droplet size monitored from satellite. *Science* **2002**, *295*, 834–838.
4. Sekiguchi, M.; Nakajima, T.; Suzuki, K.; Kawamoto, K.; Higurashi, A.; Rosenfeld, D.; Sano, I.; Mukai, S. A study of the direct and indirect effects of aerosols using global satellite datasets of aerosol and cloud parameters. *J. Geophys. Res.* **2003**, doi:10.1029/2002JD003359.

5. Matsui, T.; Masunaga, H.; Kreidenweis, S.M.; Pielke, R.A., Sr.; Tao, W.-K.; Chin, M.; Kaufman, Y.J. Satellite-based assessment of marine low cloud variability associated with aerosol, atmospheric stability, and the diurnal cycle. *J. Geophys. Res*. **2006**, doi:10.1029/2005JD006097.
6. Han, Q.; Rossow, W.B.; Zeng, J.; Welch, R. Three different behaviors of liquid water path of water clouds in aerosol-cloud interactions. *J. Atmos. Sci.* **2002**, *59*, 726–735.
7. Kaufman, Y.J.; Koren, I.; Remer, L.A.; Rosenfeld, D.; Rudich, Y. The effect of smoke, dust and pollution aerosol on shallow cloud development over the Atlantic Ocean. *Proc. Natl. Acad. Sci*. **2005**, *102*, 11207–11212.
8. Albrecht, B. Aerosols, Cloud microphysics, and fractional cloudiness. *Science* **1989**, *245*, 1227–1230.
9. Ferek, R.; Garrett, T.; Hobbes, P.V.; Strader, S.; Johnson, D.; Taylor, J.; Nielson, K.; Ackerman, A.; Kogan, Y.; Liu, Q.; *et al.* Drizzle suppression in ship tracks. *J. Atmos. Sci.* **2000**, *57*, 2707–2728.
10. Vant-Hull, B.; Marshak, A.; Remer, L.; Li, Z. The effects of scattering angle and cumulus cloud geometry on satellite retrievals of cloud drop effective radius. *Geosci. Rem. Sens. Lett.* **2007**, *45*, 1039–1045.
11. Koren, I.; Kaufman, Y.J.; Remer, L.A.; Martins, V. Measurement of the effect of Amazon smoke on inhibition of cloud formation. *Science* **2004**, *303*, 1342–1345.
12. Taubman, B.A.; Marufu, L.; Vant-Hull, B.; Piety, C.; Doddridge, B.; Dickerson, R.; Li, Z. Smoke over haze: Aircraft observations of chemical and optical properties and the effects on heating rates and stability. *J. Geophys. Res.* **2004**, doi:10.1029/2003JD003898.
13. Ackerman, A.; Toon, O.B.; Stevens, D.E.; Heymsfield, A.J.; Ramanathan, V.; Welton, E.J. Reduction of tropical cloudiness by soot. *Science* **2000**, *288*, 1042–1047.
14. Koren, I.; Kaufman, Y.J.; Rosenfeld, D.; Remer, L.A.; Rudich, Y. Aerosol invigoration and restructuring of Atlantic convective clouds. *Geophys. Res. Lett.* **2005**, doi:10.1029/2005GL023187.
15. Burnet, F.; Brenguier, J.-L. Observational study of the entrainment-mixing process in warm convective clouds. *J. Atmos. Sci.* **2007**, *64*, 1995–2011.
16. Sinclair, V.A.; Gray, S.L.; Belcher, S.E. Controls on boundary layer ventilation: Boundary layer processes and large-scale dynamics. *J. Geophys. Res.* **2010**, doi:10.1029/2009JD012169.
17. Altaratz, O.; Bar-Or, R.Z.; Wollner, U.; Koren, I. Relative humidity and its effects on aerosol optical depth in the vicinity on convective clouds. *Environ. Res. Lett.* **2013**, *8*, 34025–34030.
18. Fan, J.; Leung, L.R.; Li, Z.; Morrison, H.; Qian, Y.; Zhou, Y.; Chen, H. Aerosol impacts on clouds and precipitation in southeast China–Results from bin and bulk microphysics for the 2008 AMF-China field campaign. *J. Geophys. Res.* **2012**, doi:10.1029/2011JD016537.
19. Lebo, Z.J.; Morrison, H.; Seinfeld, J.H. Are simulated aerosol induced effects on deep convective clouds strongly dependent on saturation adjustment? *Atmos. Chem. Phys. Discuss.* **2012**, *12*, 10059–10114.
20. Wang, H.; Feingold, G. Modeling mesoscale cellular structures and drizzle in marine stratocumulus. Part I: Impact of drizzle on the formation and evolution of open cells. *J. Atmos. Sci.* **2009**, *66*, 3237–3256.
21. Lebo, Z.J.; Feingold, G. On the relationship between responses in cloud water and precipitation to changes in aerosol. *Atmos. Chem. Phys.* **2014**, *14*, 11817–11831.
22. McComiskey, A.; Feingold, G. The scale problem in quantifying aerosol indirect effects. *Atmos. Chem. Phys.* **2012**, *12*, 1031–1049

23. Storelvmo, T.; Kristjánsson, J.E.; Myhre, G.; Johnsrud, M.; Stordal, F. Combined observational and modeling based study of the aerosol indirect effect. *Atmos. Chem. Phys.* **2006**, *6*, 3583–3601.
24. Storer, R.L.; Van den Heever, S.C.; Stephens, G.L. Modeling aerosol impacts on convective storms in different environments. *J. Atmos. Sci.* **2010**, *67*, 3904–3915.
25. Ackerman, A.; Kirkpatrick, M.P.; Stevens, D.E.; Toon, O.B. The impact of humidity above stratiform clouds on indirect aerosol climate forcing. *Nature* **2004**, *432*, 1014–1017.
26. Ten Hoeve, J.E.; Remer, L.A.; Jacobson, M.Z. Biomass burning aerosol effects on clouds. *Atmos. Chem. Phys.* **2011**, *11*, 3021–3036.
27. Han, Q.Y.; Rossow, W.B.; Chou, J.; Welch, R. Global variation of cloud effective droplet concentration of low-level clouds. *Geophys. Res. Letts.* **1998**, *25*, 1419–1422.
28. Han, Q.; Rossow, W.B.; Welch, R.M.; White, A.; Chou, J. Validation of satellite retrievals of cloud microphysics and liquid water path using observations from FIRE. *J. Atmos. Sci.* **1995**, *52*, 4183–4195.
29. Andreae, M.O. Correlation between cloud condensation nuclei concentration and aerosol optical thickness in remote and polluted regions. *Atmos. Chem. Phys.* **2009**, *9*, 543–556.
30. Squires, P. The microstructure and colloidal stability of warm clouds. *Tellus* **1958**, *10*, 262–271.
31. Rosenfeld, D.; Lensky, I.M. Satellite-based insight into precipitation formation in continental and maritime convective clouds. *Bull. Am. Meteorol. Soc.* **1998**, *79*, 2457–2476.
32. Wang, M.; Ghan, S.; Liu, X.; L'Ecuyer, T.S.; Zhang, K.; Morrison, H.; Ovchinnikov, M.; Easter, R.; Marchand, R.; Chand, D.; *et al.* Constraining cloud lifetime effects of aerosols using A-Train satellite measurements. *Geophys. Res. Lett.* **2012**, doi:10.1029/2012GL052204.
33. Terai, C.R.; Wood, R.; Leon, D.C.; Zuidema, P. Does precipitation susceptibility vary with increasing cloud thickness in marine stratocumulus? *Atmos. Chem. Phys.* **2012**, *12*, 4567–4583.
34. Mann, J.A.; Chiu, J.C.; Hogan, R.J.; O'Connor, E.J.; L'Ecuyer, T.S.; Stein, T.H.M.; Jefferson, A. Aerosol impacts on drizzle properties in warm clouds from ARM Mobile Facility maritime and continental deployments. *J. Geophys. Res.* **2014**, *119*, 4136–4148.
35. Duong, H.T.; Sorooshian, A.; Feingold, G. Investigating potential biases in observed and modeled metrics of aerosol-cloud precipitation interactions. *Atmos. Chem. Phys.* **2011**, *11*, 4027–4037.
36. Feingold, G.; McComiskey, A.; Rosenfeld, D.; Sorooshian, A. On the relationship between cloud contact time and precipitation susceptibility to aerosol. *J. Geophys. Res.* **2013**, *118*, 10544–10554.
37. Wen, G.; Marshak, A.; Cahalan, R.F.; Remer, L.A.; Kleidman, R.G. 3D aerosol-cloud radiative interaction observed in collocated MODIS and ASTER images of cumulus cloud fields. *J. Geophys. Res.* **2007**, doi:10.1029/2006JD008267.
38. Mauger, G.S.; Norris, J.R. Meteorological bias in satellite estimates of aerosol cloud relationships. *Geophys. Res. Lett.* **2007**, doi:10.1029/2007GL029952.
39. Eilers, P.H.C.; Goeman, J.J. Enhancing scaterplots with smoothed densities. *Bioinformatics* **2004**, *20*, 623–628.
40. Xue, H.; Feingold, G. Large-eddy simulation of trade wind cumuli: Investigation of aerosol indirect effects. *J. Atmos. Sci.* **2006**, *63*, 1605–1622.
41. Bony, S.; Dufresne, J.-L. Marine boundary layer clouds at the heart of tropical cloud feedback uncertainties in climate models. *Geophys. Res. Lett.* **2006**, *32*, L20806.

42. Tao, W.K.; Chen, J.P.; Li, Z.Q.; Wang, C.; Zhang , C.D. Impact of aerosols on convective clouds and precipitation. *Rev. Geophys.* **2012**, doi:10.1029/2011RG000369.